

Reliability of the optimized perturbation theory in the 0-dimensional $O(N)$ scalar field model

Dérick S. Rosa,^{1,*} R. L. S. Farias,^{2,3,†} and Rudnei O. Ramos^{4,‡}

¹*Instituto de Física Teórica, Universidade Estadual Paulista, 01140-070 São Paulo, SP, Brazil*

²*Departamento de Física, Universidade Federal de Santa Maria, 97105-900, Santa Maria, RS, Brazil*

³*Department of Physics, Kent State University, Kent, OH 44242, United States*

⁴*Departamento de Física Teórica, Universidade do Estado do Rio de Janeiro, 20550-013 Rio de Janeiro, RJ, Brazil*

We address the reliability of the Optimized Perturbation Theory (OPT) in the context of the 0-dimensional $O(N)$ scalar field model. The effective potential, the self-energy and the 1PI four-point Green's function for the model are computed using different optimization schemes and the results contrasted to the exact results for the model. Our results are also compared to those obtained with the $1/N$ -expansion and with those from ordinary perturbation theory. The OPT results are shown to be stable even at large couplings and to have better convergence properties than the ones produced in the $1/N$ -expansion. It is also shown that the principle of minimal sensitive optimization procedure used in conjunction with the OPT method tends to always produce better results, in particular when applied directly to the self-energy.

PACS numbers: 12.38.Lg, 11.80.Fv, 11.15.Tk

I. INTRODUCTION

Perturbation theory is the most comprehensive way of studying nonlinear problems in physics area wide. However, it is a fact that not always we can rely on some small quantity in the theory which we can use as a parameter which we can perturb physical quantities of interest, or even when we do have, it is not warranted that a perturbative series might be well posed, i.e., converge after a few terms are considered. Most of the times we must make use of some nonperturbative method to get around these problems. One typical example where perturbation theory breaks down is in the studies of phase transitions in general, particularly close to a critical point. This can also happen due to the appearance of large infrared divergences [1], as in the case where massless modes are present, or close to a transition point in field theories displaying a second order phase transition [2] or a weakly first order transition [3]. In all these cases, the use of some reliable nonperturbative technique is required to properly study these systems. Among the analytical nonperturbative techniques, one can cite for example making use of a discretization of the system and studying it numerically (e.g., lattice simulations), make use of analytical methods like an expansion in the number of field components, N , in the case of field theory, using the $1/N$ -approximation [4], among other methods.

In this work we want to access the reliability of one of those nonperturbative methods that have been used with some frequency in the literature: The optimized perturbation theory (OPT). The OPT is an analytical technique which allies the computational advantages of

ordinary perturbation theory to a variational criterion in order to generate nonperturbative results [5]. The OPT method has been used extensively in the literature to treat many different physical systems, ranging from condensed matter problems, phase transition problems in finite temperature quantum field theory and others (see, e.g., Refs. [6–21] and references there in for some examples of applications).

One particular issue regarding the OPT method that we would like to also address in this work regards the quantity to which one should apply the variational criterion as required by the method. In a calculation where different physical quantities are available, in the original proposal by Stevenson [22], the variational principle used was the principle of minimal sensitivity (PMS) and it was advocated that the PMS should be applied to each different physical quantity that is being computed, producing different optimized parameters. However, one could argue that the PMS should be applied to a more general quantity such as the ground-state energy density as in Ref. [23], or to the effective potential, which generates all one-particle irreducible contributions, as in Ref. [11–14, 24], while previous works [25, 26] have shown that applying the PMS to the self-energy would be more appropriate. In this work we want to clarify in this issue of which quantity we should optimize in the OPT method and also which quantity can provide the best convergence in the OPT. With this aim we shall compare the results obtained by a direct optimization of the effective potential (the zero-point Green function), the self-energy (the two-point Green function) and also to the effective coupling (the four-point Green function) in the context of the 0-dimensional $O(N)$ scalar field theory model. As an exact soluble model, it makes the perfect benchmark toy model to test different nonperturbative methods used in quantum field theory [27].

The remainder of this work is organized as follows. In Sec. II, we briefly describe the 0-dimensional $O(N)$ scalar

*Electronic address: derick@ift.unesp.br

†Electronic address: rfarias@kent.edu

‡Electronic address: rudnei@uerj.br

field model and show why perturbation theory might not be reliable in the context of this model in special. In Sec. III, we introduce the OPT method and also describe three main variational tools that are commonly used in conjunction with this method. In Sec. IV, we perform a comparison between exact results and the nonperturbative results obtained by OPT. These results are also contrasted with those obtained from the $1/N$ -expansion. This way we can better evaluate the usefulness of the OPT and the corresponding variational methods with this popular nonperturbative method. Our concluding remarks are given in Sec. V. Three appendixes are included where we give some of the technical details.

II. THE 0-DIMENSIONAL $O(N)$ SCALAR FIELD MODEL

The 0-dimensional $O(N)$ scalar field model describes an N -component anharmonic oscillator in zero spacetime dimension, whose action is given by

$$S(\varphi) = \frac{m}{2}\varphi \cdot \varphi + \frac{\lambda}{4!}(\varphi \cdot \varphi)^2, \quad (2.1)$$

where m, λ are real and positive parameters and $\varphi \equiv (\varphi_1, \dots, \varphi_N)$ is a scalar field with N components. Equation (2.1) is an invariant under $O(N)$ rotations.

The generating function for the n -point Green's functions is given by

$$Z(\mathbf{J}) = \int D\varphi \exp[-S(\varphi) + \mathbf{J} \cdot \varphi], \quad (2.2)$$

where \mathbf{J} is an external source. From the generating function, the n -point Green functions are given by

$$G_{i_1 \dots i_n}^{(n)} = \frac{1}{Z} \frac{\delta^n Z(\mathbf{J})}{\delta J_{i_1} \dots \delta J_{i_n}} \Big|_{J_i=0} = \langle \varphi_{i_1} \dots \varphi_{i_n} \rangle, \quad (2.3)$$

and averages are given by their standard definition,

$$\langle \dots \rangle = \frac{\int D\varphi \exp[-S(\varphi)] [\dots]}{Z}. \quad (2.4)$$

The connected Green functions are obtained from the functional generator $W(\mathbf{J})$, defined as [28]

$$W(\mathbf{J}) = \ln \left[\frac{Z(\mathbf{J})}{Z_0} \right], \quad (2.5)$$

where Z_0 is the normalization of the generating functional $Z_0 = Z(\mathbf{J} = 0)|_{\lambda=0}$. The connected Green functions are then given by

$$G_{c, i_1 \dots i_n}^{(n)} = \frac{\delta^n W(\mathbf{J})}{\delta J_{i_1} \dots \delta J_{i_n}} \Big|_{J_i=0} = \langle \varphi_{i_1} \dots \varphi_{i_n} \rangle_{\text{connected}}. \quad (2.6)$$

From the definition of the expectation value of the field,

$$\phi_i = \langle \varphi_i \rangle_{J_i} = \frac{\delta W}{\delta J_i}, \quad (2.7)$$

we can perform the usual Legendre transformation and obtain the effective action, or the generation functional of the one-particle irreducible (1PI) Green's functions [28]

$$\Gamma(\phi) = W(\mathbf{J}) - \mathbf{J} \cdot \phi. \quad (2.8)$$

The advantage of working with the 0-dimensional $O(N)$ scalar field model is that it has explicit analytical solution, which can be contrasted with different approximations used in the literature and, thus, it is a perfect benchmarking model to use. In this work, we will make use of the effective potential V_{eff} , the self-energy Σ and the 1PI four-point Green's functions. The one-particle irreducible (1PI) Green's functions, $\Gamma^{(n)}$, are defined by

$$\Gamma_{i_1 \dots i_n}^{(n)} = - \frac{\delta^n \Gamma[\phi]}{\delta \phi_{i_1} \dots \delta \phi_{i_n}} \Big|_{\phi=0} \quad (2.9)$$

In particular, in the rest of this work we will make use of the effective potential, $V_{\text{eff}} = -\ln Z$, the self-energy, $\Sigma \equiv \Gamma^{(2)} - m$ and the vertex function $\Gamma^{(4)}$.

Let us give the explicit expressions for these quantities for the present model. Starting with the partition function, $Z \equiv Z(0)$, given by [27, 29]

$$Z = \int \mathcal{D}\varphi e^{-S(\varphi)} = \Omega_N \mathcal{R}_{N-1}, \quad (2.10)$$

where Ω_N is the surface area in N -dimensional unit sphere,

$$\Omega_N = \frac{2\pi^{N/2}}{\Gamma\left(\frac{N}{2}\right)}, \quad (2.11)$$

and \mathcal{R}_N is defined by

$$\begin{aligned} \mathcal{R}_N &= \int_0^\infty x^N e^{-\frac{m}{2}x^2 - \frac{\lambda}{4!}x^4} dx \\ &= 2^{\frac{3N-5}{4}} 3^{\frac{N+1}{4}} \lambda^{-\frac{N+3}{4}} \left[\sqrt{\lambda} \Gamma\left(\frac{N+1}{4}\right) \right. \\ &\quad \times {}_1F_1\left(\frac{N+1}{4}; \frac{1}{2}; \frac{3m^2}{2\lambda}\right) - \sqrt{6}m\Gamma\left(\frac{N+3}{4}\right) \\ &\quad \left. \times {}_1F_1\left(\frac{N+3}{4}; \frac{3}{2}; \frac{3m^2}{2\lambda}\right) \right], \end{aligned} \quad (2.12)$$

where ${}_1F_1(\alpha; \beta; z)$ is the Kummer confluent hypergeometric function [30].

The explicit exact solutions for V_{eff} , Σ and $\Gamma^{(4)}$ that we use throughout this work are then found to be given, respectively, by:

$$V_{\text{eff}}^{\text{exact}} = -\log(\Omega_N \mathcal{R}_{N-1}), \quad (2.13)$$

$$\Sigma_{\text{exact}} = N \frac{\mathcal{R}_{N-1}}{\mathcal{R}_{N+1}} - m, \quad (2.14)$$

$$\Gamma_{\text{exact}}^{(4)} = -3N^2 \left(\frac{\mathcal{R}_{N-1}}{\mathcal{R}_{N+1}} \right)^2 \left[\frac{N(\mathcal{R}_{N+3})(\mathcal{R}_{N-1})}{(N+2)(\mathcal{R}_{N+1})^2} - 1 \right] \quad (2.15)$$

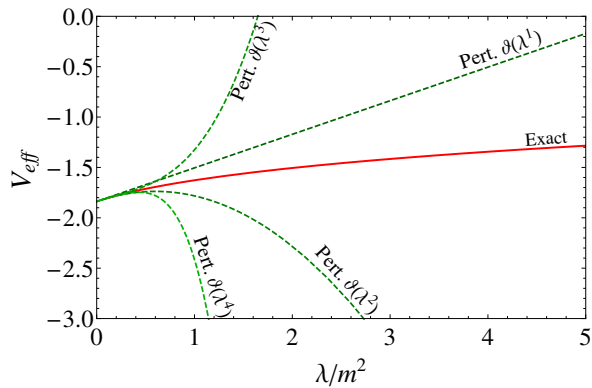


Figure 1: The effective potential V_{eff} for the model, considering $N = 2$. The exact solution is given by the solid line. The results obtained by expanding V_{eff} in a power series in λ/m^2 are given by the dashed lines.

For illustrative purposes, we give in Appendix A the perturbative expansion (the power series expansion in the coupling constant λ) for the effective potential, V_{eff} , the self-energy Σ and the vertex function $\Gamma^{(4)}$. That this is not a well posed perturbative series (as far convergence is concerned) is shown in Fig. 1 for the particular case of the perturbative expansion for the effective potential. We can see that perturbative expansion shows no sign of converging. In fact, it can be shown that the series has a zero radius of convergence [31].

III. OPTIMIZED PERTURBATION THEORY

The application of the OPT method starts by implementing a linear interpolation in the action,

$$S \rightarrow S_\delta = (1 - \delta) S_0(\eta) + \delta S, \quad (3.1)$$

where δ is a fictitious expansion parameter, which is used only for bookkeeping purposes and set at the end equal to one. The parameter η is an arbitrary mass term, fixed through an appropriate variational method.

Some common ways of fixing this parameter will be described below. It is through this variational method that nonperturbative effects are included through the OPT mass parameter η . The OPT method has been successfully applied in different scenarios (see, e.g Refs. [6–14, 32, 33] and references there in). In this work, we apply this nonperturbative method to evaluate the n -point 1PI Green's functions of the 0-dimensional $O(N)$ scalar field model described in the previous section. We compare the OPT results with the exact solution that this particular toy model gives. For comparison purposes we also contrast the OPT results with those obtained through another nonperturbative method, obtained with the $1/N$ -expansion for the model.

Applying the interpolation (3.1) in Eq. (2.1) gives

$$\begin{aligned} S(\varphi) &= \frac{m}{2} \varphi \cdot \varphi + (1 - \delta) \frac{\eta}{2} \varphi \cdot \varphi + \delta \frac{\lambda}{4!} (\varphi \cdot \varphi)^2 \\ &= S_0(\varphi, \eta) + S_\delta(\varphi, \eta), \end{aligned} \quad (3.2)$$

where

$$S_0(\varphi, \eta) = \frac{m + \eta}{2} \varphi \cdot \varphi, \quad (3.3)$$

and

$$S_\delta(\varphi, \eta) = -\delta \frac{\eta}{2} \varphi \cdot \varphi + \delta \frac{\lambda}{4!} (\varphi \cdot \varphi)^2, \quad (3.4)$$

which is considered as the modified interaction term in the OPT method.

The generating functional, using Eq. (3.2), becomes

$$Z = \int \mathcal{D}\varphi e^{-S_0(\varphi, \eta)} e^{-S_\delta(\varphi)}. \quad (3.5)$$

The strategy to evaluate the effective potential $V_{\text{eff}} = -\ln Z$, Σ and $\Gamma^{(4)}$ using OPT is very similar as we would do when using perturbation theory. Using the interaction term (3.4), we can compute the physical quantity of interest expanding the result up to some order k in δ . The procedure is immediate if we use the exact expressions Eqs. (2.13), (2.14) and (2.15), by making the substitutions in those expressions, $m \rightarrow m + (1 - \delta)\eta$, $\lambda \rightarrow \delta\lambda$ and then expanding the respective expression up to the desired order in δ . For example, the effective potential, evaluated up to order δ^2 , is given by

$$\begin{aligned} V_{\text{eff}} &= -\ln \left[\frac{2^N \pi^{N/2} (m + \eta)^{-N/2} \Gamma(1 + \frac{N}{2})}{N \Gamma(\frac{N}{2})} \right] \delta^0 \\ &+ N \left[\frac{\lambda(2 + N) - 12\eta(m + \eta)}{24(m + \eta)^2} \right] \delta^1 \\ &- \left\{ N \left[\frac{36\eta^2(m + \eta)^2 - 12\lambda(2 + N)\eta(m + \eta)}{144(m + \eta)^4} \right] \right. \\ &\left. + N \left[\frac{\lambda^2(6 + 5N + N^2)}{144(m + \eta)^4} \right] \right\} \delta^2 + \mathcal{O}(\delta^3). \end{aligned} \quad (3.6)$$

Likewise, the self-energy in the OPT (up to order δ^2) is given by

$$\begin{aligned} \Sigma &= \eta \delta^0 + \left[\frac{\lambda(2+N) - 6\eta(m+\eta)}{6(m+\eta)} \right] \delta^1 \\ &\quad - \left[\frac{\lambda(2+N) [\lambda(4+N) - 6\eta(m+\eta)]}{36(m+\eta)^3} \right] \delta^2 \\ &\quad + \mathcal{O}(\delta^3), \end{aligned} \quad (3.7)$$

and $\Gamma^{(4)}$ (up to order δ^2) is given by

$$\Gamma^{(4)} = \lambda \delta^1 - \left[\frac{\lambda^2(8+N)}{6(m+\eta)^2} \right] \delta^2 + \mathcal{O}(\delta^3). \quad (3.8)$$

High order terms for V_{eff} , Σ and $\Gamma^{(4)}$ can be founded in Appendix B. Note that these expressions expressed as a power series in δ they depend explicitly on the OPT parameter η . This parameter is fixed using an appropriate variational principle, as we explain next.

A. Optimization procedures

If we would perform the expansion in δ to all orders, then after taking the limit $\delta \rightarrow 1$, of course the η dependence of the quantities would exactly cancel. However, this expansion to all orders is impracticable. In other words, we need to eventually truncate the series at some order k in δ . This means that a η dependence is left in the results and this parameter need to be fixed somehow. In this work, we will study three possible optimization procedures used to fix η in the OPT method: The Principle of Minimal Sensitivity (PMS), the Fastest Apparent Convergence (FAC) and, finally, the Turning Point (TP) method. The PMS is based on a variational principle [22]. If a physical quantity Φ does not depend originally on η , we must then determine the value of η that makes this quantity minimally sensitive to it. This is the basis for the PMS method, which is then determines η by requiring that the quantity Φ evaluated to some order k in δ , $\Phi^{(k)}$, must satisfy

$$\left. \frac{d\Phi^{(k)}}{d\eta} \right|_{\eta=\bar{\eta}, \delta=1} = 0. \quad (3.9)$$

The PMS then provides a new mass term $\bar{\eta}$ that depends on the original parameters of the theory, e.g., the coupling constants, thus bringing in the nonperturbative results. We must emphasize that it is not always guaranteed the existence of nontrivial solution for the PMS Eq. (3.9) and we need to verify this in each PMS application. When it is the case that we cannot find a solution, then we need to make use of some other optimization procedure. For example, in the FAC procedure [34]), we require that the k_{th} -coefficient of the expansion in δ of a physical quantity Φ ,

$$\Phi^{(k)} = \sum_{i=0}^k c_i \delta^i, \quad (3.10)$$

to satisfy

$$\left. \left[\Phi^{(k)} - \Phi^{(k-1)} \right] \right|_{\delta=1} = 0. \quad (3.11)$$

This condition is, thus, equivalent to taking the k_{th} -coefficient in Eq. (3.10) equal to zero. One should note that it is not at all guaranteed that the condition given by either Eq. (3.9) or by Eq. (3.10) might have necessarily a nontrivial solution. Then a third method can be used. As proposed in Ref. [35], in the cases that neither of the PMS or the FAC have a solution, then we can make use of the TP method. The TP method is defined by the condition [35]

$$\left. \frac{d^2\Phi^{(k)}}{d\eta^2} \right|_{\eta=\bar{\eta}, \delta=1} = 0. \quad (3.12)$$

In the next section we will study the nonperturbative OPT results applied to the model explained in Sec. II. We make a comparison of the OPT results with those obtained from an expansion in the number of components for the field, i.e., the large- N (LN) expansion, which is explained in the Appendix C and we also compare these results with those obtained from the exact solution for the model.

IV. RESULTS

In this section we will present our results using the OPT when evaluating the effective potential V_{eff} , the self-energy Σ and the vertex function $\Gamma^{(4)}$ for the 0-dimensional scalar field model. These results are also contrasted with the ones obtained using the LN expansion, presented in Appendix C (see also Ref. [27] for details).

In Fig. 2 we show the results for the effective potential V_{eff} at $N = 2$ in the cases of both the OPT and LN. Contrary to the results obtained in perturbation theory and shown in Fig. 1, we see from the results in Fig. 2 that the OPT and LN both produce results with better convergence properties, with the OPT at order δ^2 already agreeing quite well with the exact result. This agreement remains even when the coupling is much larger, while the LN results, at increasing orders in $1/N$, tend to oscillate around the exact solution.

Results for self-energy Σ at $N = 2$ are presented in Fig. 3. In the panel (a) of Fig. 3 we can again see the bad behavior of perturbation theory. In this same panel,

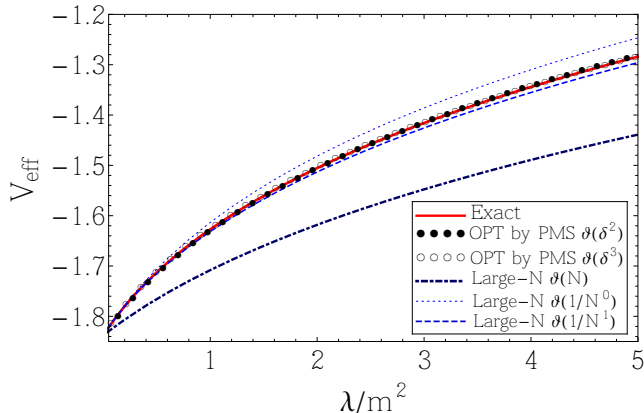


Figure 2: The effective potential V_{eff} for $N = 2$. The exact result (solid line), the LN results (dashed-dotted, dotted and dashed lines) and the OPT results (circles), where we optimize Σ by using the PMS condition.

we also show the results for the LN for this case, while in the panel (b) of Fig. 3 we show both the LN result at order $1/N^2$ and the OPT at analogous order, δ^2 . Again we see that the OPT covers much better the exact result even for very large values for the coupling constant. Here we have optimized Σ by PMS (note that PMS and TP do not present nontrivial solutions at $\mathcal{O}(\delta^1)$, while the results from FAC are slight worse than the ones obtained with the PMS).

Results for $\Gamma^{(4)}$ are presented in Fig. 4. In the panel (a) of Fig. 4 we show once again the breakdown of perturbation theory, while the LN results present strong deviations from the exact result. In the panel (b) of Fig. 4 we show how by increasing the order in the OPT it oscillates around the exact solution, converging to it. In this case we optimize Σ by PMS and use the solution in $\Gamma^{(4)}$. The other optimization schemes, FAC and TP produce results that are worse. Choosing to optimize the effective potential, or the own function $\Gamma^{(4)}$ also lead to results that worse than optimizing the self-energy and using the result back in $\Gamma^{(4)}$. This shows that for this case, optimizing the self-energy as a basic quantity, in the PMS scheme, is the better choice.

In Fig. 5 we verify how the dependence on N influences the results for the effective potential. Three cases are considered, $N = 2$, $N = 4$ and $N = 10$ and both OPT and LN are contrasted with the exact solution. In this case, as we have adopted in Fig. 2, we have chosen to optimize Σ using the PMS so to get the optimum solution $\bar{\eta}$ and this solution is then used back in V_{eff} . Once again, the PMS applied on the self-energy is found to be the best optimization scheme. The results presented in Fig. 5 also show that in general the OPT presents more robust results than the LN approximation, with the OPT converging faster to the exact result.

In Figs. 6 and 7 we also study the dependence of the different methods as a function of the number of components N , for the fixed value of the parameters in the model, $\lambda/m^2 = 1$, for the self-energy Σ and coupling function $\Gamma^{(4)}$, respectively. In Fig. 6, where we show the self-energy Σ as a function of N , we can see that the LN results tend to present convergence to the exact solution only for very large values of N . As in the OPT case, when optimizing the own self-energy Σ using the PMS scheme, it shows results that are much weaker dependent on N , as far the convergence is concerned. The result from the OPT are also much closer to the exact solution. For comparison purposes, we also show in the panel (b) of Fig. 6 the results obtained using the FAC optimization procedure (applied on Σ), which also presents a very small deviation from the exact solution, even for larger values of N , but it slight under estimates the exact solution when compared with the PMS optimization procedure.

Likewise, in Fig. 7 we show the results for $\Gamma^{(4)}$ as a function of N for the different approximation methods. In the panel (a) of Fig. 7 we give the LN results, while in the panel (b) we give the OPT results. We note that LN results present a strong deviation from the exact solution, only tending to converge (in an oscillatory manner) at very larger values of N , while the OPT results are robust at any order in N and presents very good with the exact solution already at $\mathcal{O}(\delta^3)$.

In Fig. 8 we show how the different optimization schemes within the OPT, the PMS, FAC and TP, affect the result for V_{eff} . It is also compared the results by applying those optimization schemes either to the effective potential itself, or to the self-energy and using the produced optimal value of η back in the effective potential. These results show that the best agreement with the exact solution is obtained by optimizing Σ with PMS. The same is repeated when we evaluate the self-energy Σ , whose results are shown in Fig. 9, and for the 1PI four point function $\Gamma^{(4)}$, shown in Fig. 10. In all these cases, the best converging results are obtained when we choose to optimize the self-energy in the PMS scheme.

Let us better quantify the differences between the two nonperturbative methods studied in this work, the OPT and the LN approximation. We want also to quantify the differences between the different optimization schemes. This is done next, where we analyze the percentage difference that each method produces. We define the percentage difference as

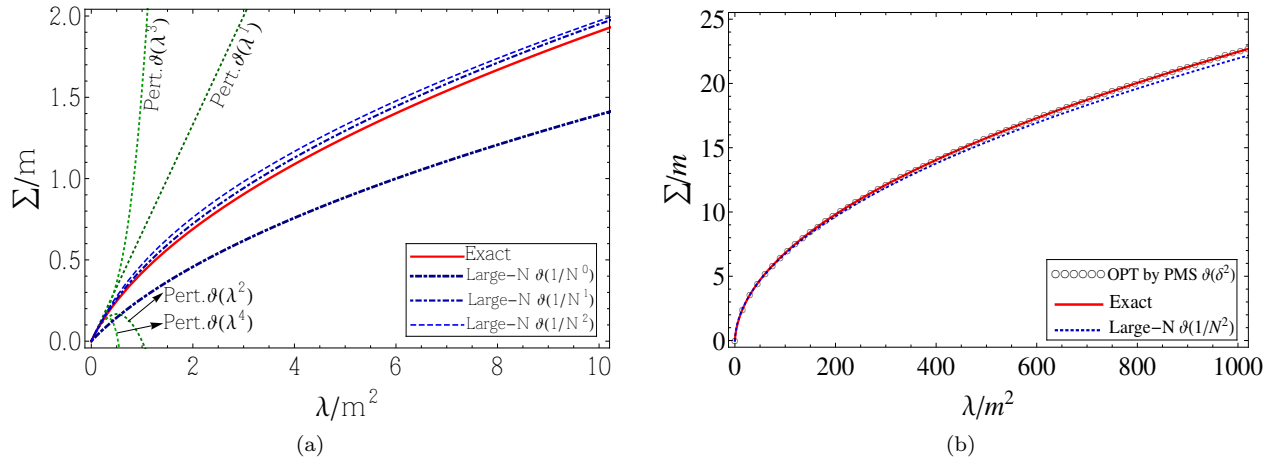


Figure 3: The self-energy Σ for $N = 2$. Panel (a): The exact result (solid line), LN results (dotted and dashed-dotted lines) and the perturbative results (dotted lines) as a function of the coupling constant. Panel (b): Extrapolation of the results for the strong coupling regime, for the cases of LN result, shown to $\mathcal{O}(\frac{1}{N^2})$ (dashed line), exact result (solid line) and OPT result (circle), shown to $\mathcal{O}(\delta^2)$ optimizing Σ by PMS.

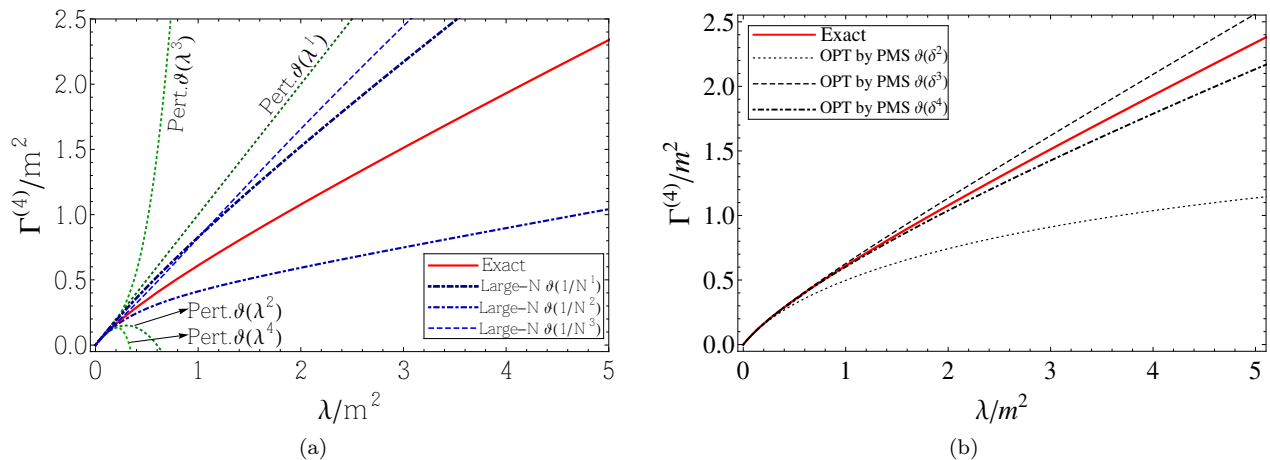


Figure 4: Results for $\Gamma^{(4)}$ for $N = 2$. Panel (a): the perturbative results (dotted lines), the LN results (dashed and dashed-dotted lines) and the exact solution (solid line). Panel (b): The exact solution (solid line) and the OPT results shown up to $\mathcal{O}(\delta^4)$, which were obtained by optimizing Σ using the PMS scheme.

$$\Phi_{\%} = \left| \frac{\Phi_{\text{exact}} - \Phi_{\text{approximated}}}{\Phi_{\text{exact}}} \right|, \quad (4.1)$$

where Φ can represent any physical quantity evaluated in this work: V_{eff} , Σ or $\Gamma^{(4)}$. In Figs. 11, 12 and 13 we show the percentage difference for Σ , V_{eff} and $\Gamma^{(4)}$, respectively. Panel (a) in these figures always refers to the OPT results, where, based on the previous results, we have chosen to optimize the self-energy in the two schemes that performs well, the PMS and the FAC schemes. The results shown in panel (b) show the analogous percentage difference of the approximation compared to the exact so-

lution, but for the LN approximation. For convenience, we have chosen two fixed values for N , $N = 2$ and $N = 4$. We can see that the OPT results are quite impressive, showing good convergence in most cases already at second order, while the LN results present strong deviations from the exact solution. In particular, we can see that the OPT provides excellent results for Σ and V_{eff} , but for $\Gamma^{(4)}$ it is necessary to go to higher orders in δ . As we expected, if we increase the value of N LN presents better results, but still it under performs when compared with the OPT results.

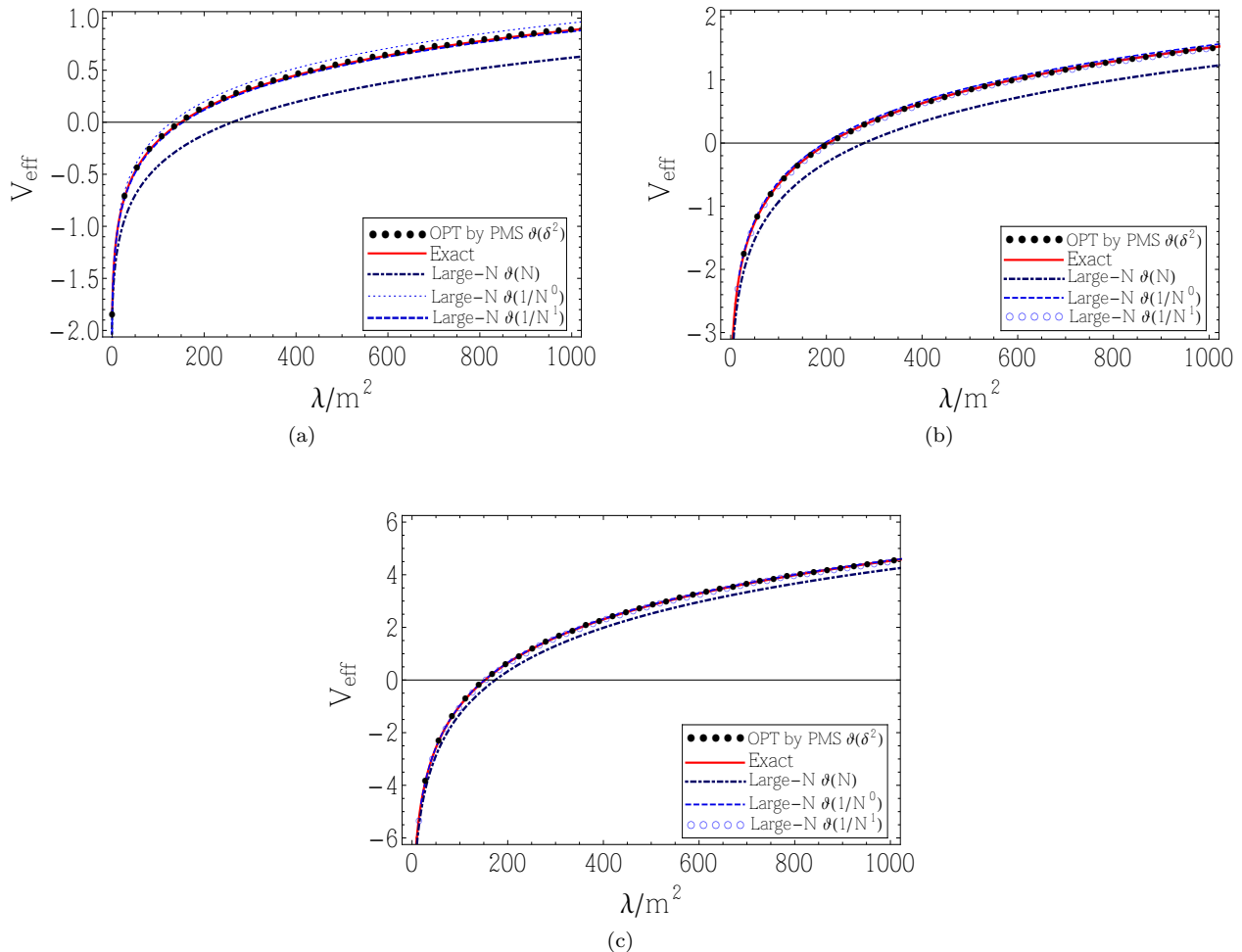


Figure 5: Results for the effective potential V_{eff} for the cases of $N = 2$ (panel (a)), $N = 4$ (panel (b)) and for $N = 10$ (panel (c)). The exact solution is shown with a solid line, the LN results are given by the dashed-dotted, dashed and unfilled circles and the OPT results are represented by filled circles, shown up to $\mathcal{O}(\delta^2)$. The choice here was to optimize Σ using the PMS scheme.

V. CONCLUSIONS

In this work we have investigated in details the application of the OPT in the 0-dimensional $O(N)$ scalar field model. The questions we wanted to answer with these work were, which optimization scheme works better with the OPT and which quantity should we optimize to obtain the optimum mass parameter that the OPT makes use to generate nonperturbative results. Through this study, we were able to better access the convergence of the OPT with respect to the different optimization schemes and with respect to each physical quantity that they should be applied (for earlier studies on the convergence of the OPT in the context of the anharmonic

potential, see, e.g., Ref. [33], while for a critical theory in field theory, Ref. [36]). Through the results obtained, we have reached the conclusion that the PMS applied to the self-energy is in general be best choice for producing results with better and faster convergence.

One of the main advantages of the OPT method is its easy implementation, that follows in practice the standard perturbative expansion, but still able to generate nonperturbative results when complemented with a proper optimization procedure. In this work, we have better clarified which optimization procedure is the ideal and to which physical quantity it should be applied. For comparative purposes, we have contrasted the results obtained with the OPT method with another popular non-perturbative scheme, the LN expansion. Our results have shown that the OPT is not only competitive but also outperforms the results obtained with the LN method. Despite the simplicity of the model we have used in this

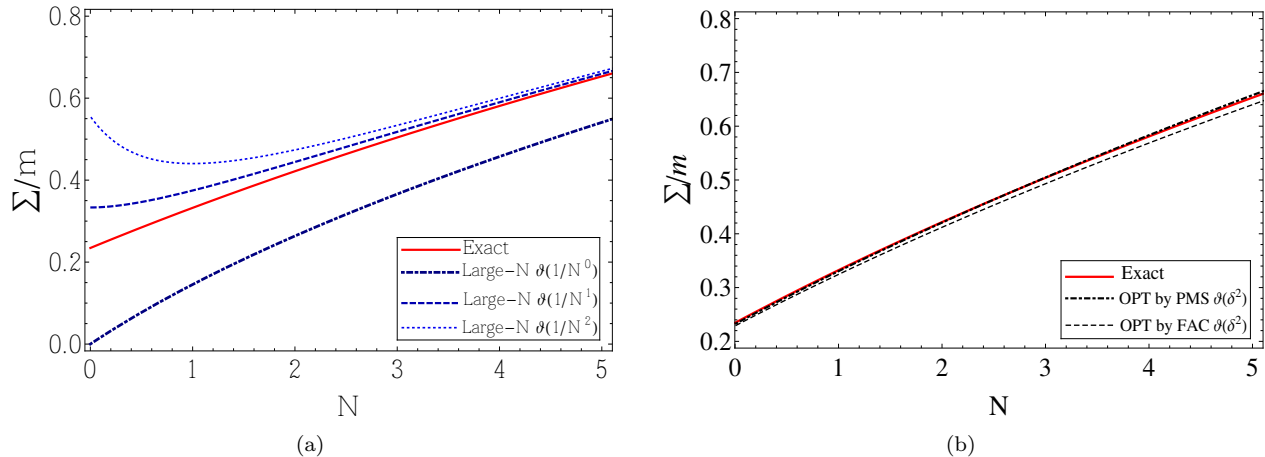


Figure 6: Results for Σ , for a fixed value of $\frac{\lambda}{m^2} = 1$, as function of N . Panel (a): The exact solution (solid line) and the LN results. panel (b): The exact solution (solid line) and the OPT results to $\mathcal{O}(\delta^2)$ and $\mathcal{O}(\delta^3)$, obtained by optimizing Σ by PMS (dotted-dashed) and by FAC (dashed).

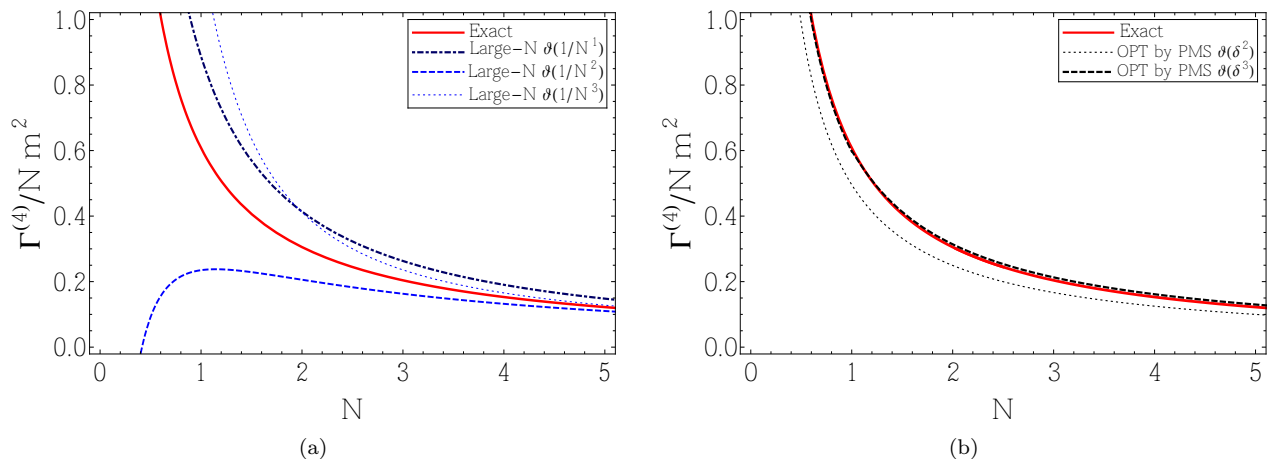


Figure 7: Results for the four point function $\Gamma^{(4)}$, at the fixed value $\frac{\lambda}{m^2} = 1$, as function of N . Panel (a): The exact solution (solid line) and the LN results (dashed, dashed-dotted and dotted lines). Panel (b): The OPT results to $\mathcal{O}(\delta^2)$ and $\mathcal{O}(\delta^3)$, obtained by optimizing Σ by PMS.

study, our results indicate that the OPT method can indeed be a better and simpler alternative when applied to theories in physical dimensions $D > 0$. Our results are then expected to better motivate the use of the OPT method as a powerful nonperturbative technique, specially when combined with appropriate optimization schemes (for recent advances on the OPT method and its combination also with renormalization group techniques, see, e.g., Refs. [37–39]).

Acknowledgments

This work was partially supported by CAPES, CNPq, FAPERJ (Brazilian funding agencies). R.L.S.F. acknowledges the kind hospitality of the Center for Nuclear Research at Kent State University, where part of this work has been done.

Appendix A: Perturbation Theory

In this appendix we present some results obtained when we use perturbation theory to evaluate the Green's

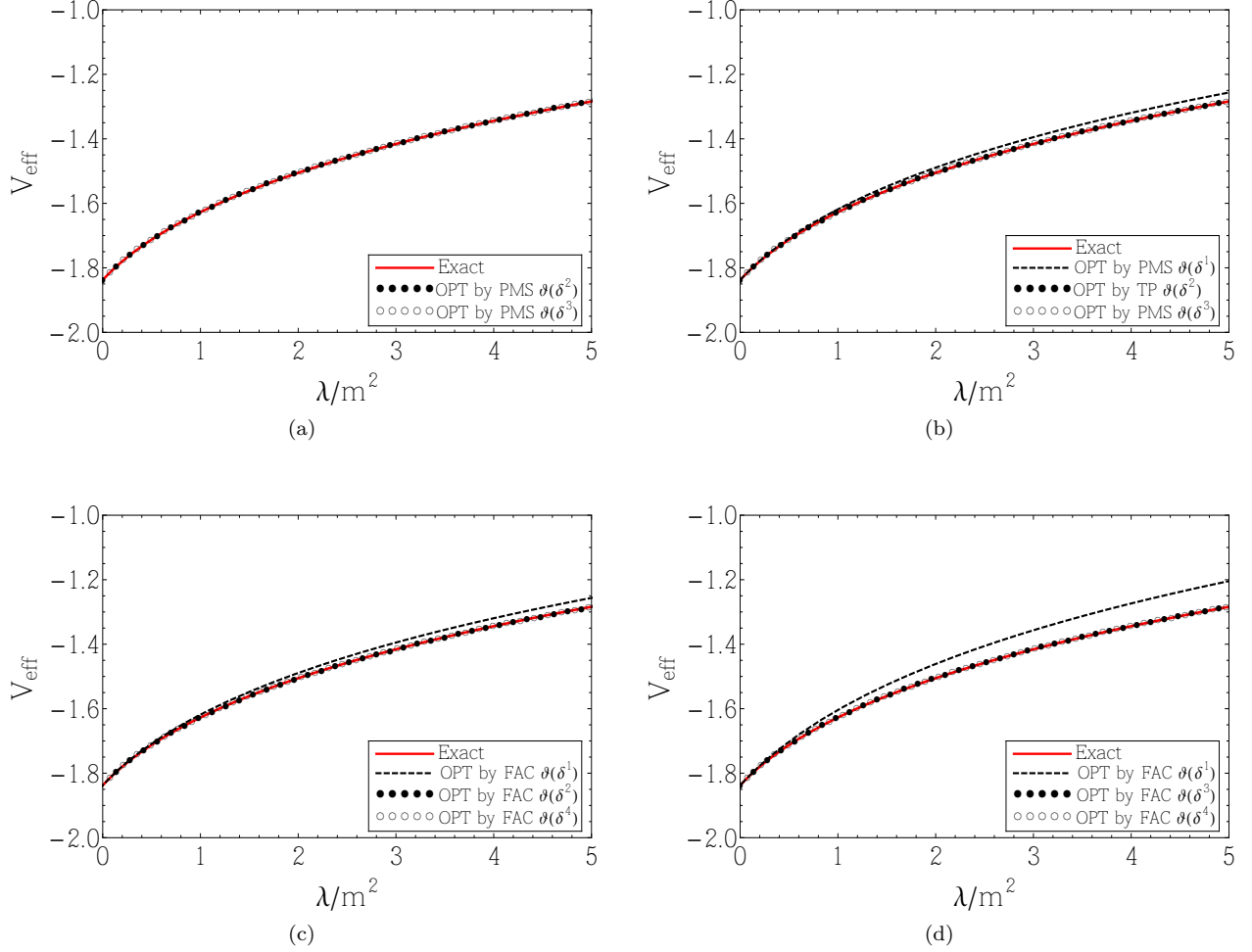


Figure 8: Exact result (solid line) and OPT results (dashed line and circles) for V_{eff} at $N = 2$ when we optimize: Σ by PMS (panel (a)), V_{eff} by PMS and TP (panel (b)), Σ by FAC (panel (c)) and V_{eff} by FAC (panel (d)).

functions for the 0-dimensional $O(N)$ scalar field model. The usual strategy is to expand the interaction term of the partition function in powers of the coupling constant λ and then use hyperspherical coordinates to evaluate the generating functional at each order in perturbation theory. For higher orders in the perturbative expansion, we can use the Feynman rules for the model (for further

details, see, e.g., Ref. [27]).

The (non normalized) effective potential V_{eff} for this model can be defined as $V_{\text{eff}} = -\ln Z$. The effective potential evaluated in perturbation theory up to $\mathcal{O}\left(\frac{\lambda}{m^2}\right)^6$ is

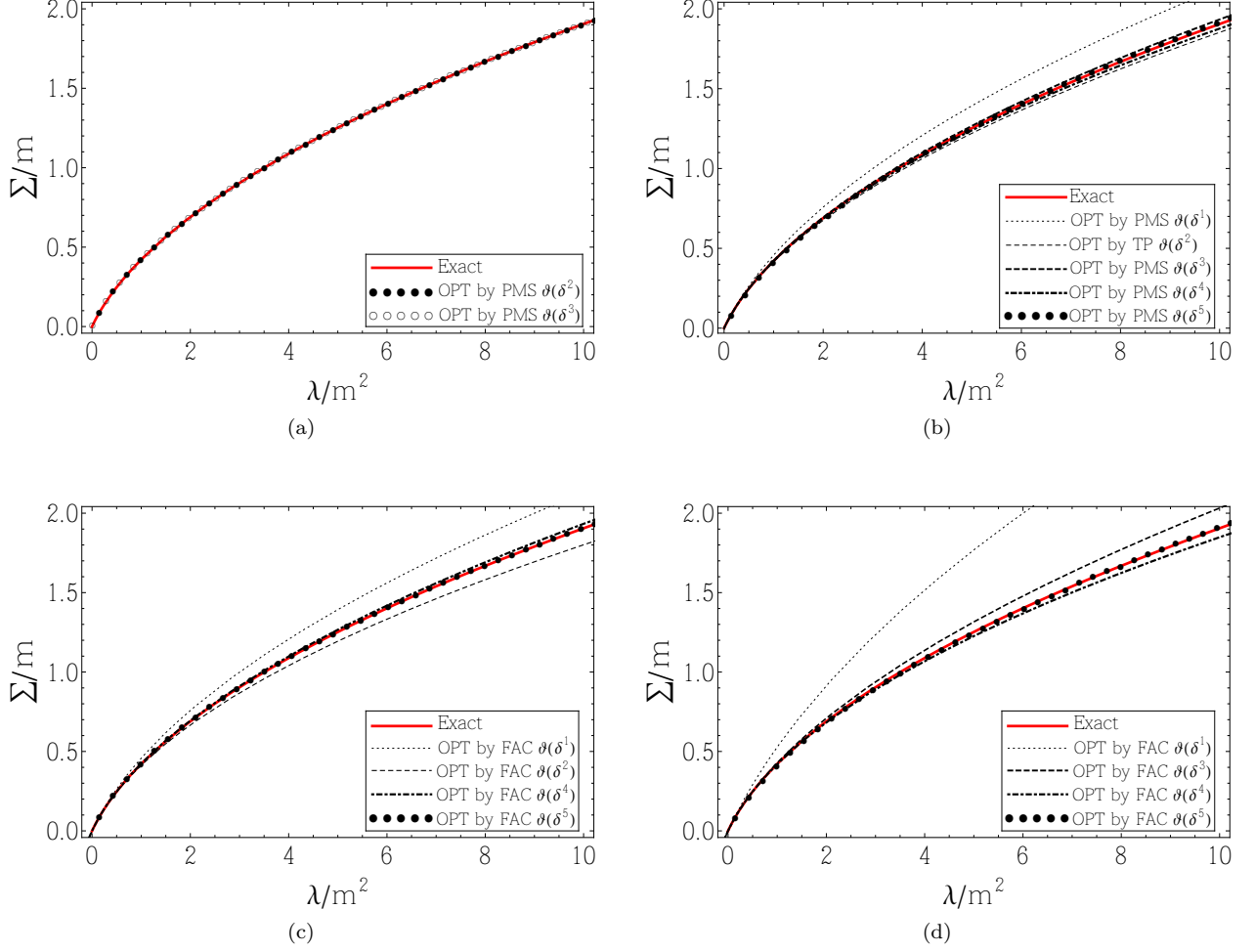


Figure 9: Exact result (solid line) and OPT results for Σ at $N = 2$ when we optimize: Σ by PMS (panel (a)), V_{eff} by PMS and TP (panel (b)), Σ by FAC (panel (c)) and V_{eff} by FAC (panel (d)).

$$\begin{aligned}
V_{\text{eff}} = & -\ln \left[\frac{2^{N-1} \pi^{N/2}}{m^{N/2}} \right] + \frac{N^2 + 2N}{24} \left(\frac{\lambda}{m^2} \right) - \frac{N^3 + 5N^2 + 6N}{144} \left(\frac{\lambda}{m^2} \right)^2 \\
& + \frac{5N^4 + 44N^2 + 128N^2 + 120N}{2592} \left(\frac{\lambda}{m^2} \right)^3 \\
& - \frac{7N^5 + 93N^4 + 468N^3 + 1040N^2 + 840N}{10368} \left(\frac{\lambda}{m^2} \right)^4 \\
& + \frac{21N^6 + 386N^5 + 2900N^4 + 11000N^3 + 20712N^2 + 15120N}{77760} \left(\frac{\lambda}{m^2} \right)^5 \\
& - \frac{33N^7 + 793N^6 + 8178N^5 + 45900N^4 + 146000N^3 + 245352N^2 + 166320N}{279936} \left(\frac{\lambda}{m^2} \right)^6 + \mathcal{O} \left(\left(\frac{\lambda}{m^2} \right)^7 \right) \quad (\text{A1})
\end{aligned}$$

The results for the self-energy Σ and $\Gamma^{(4)}$ are, respectively, given by

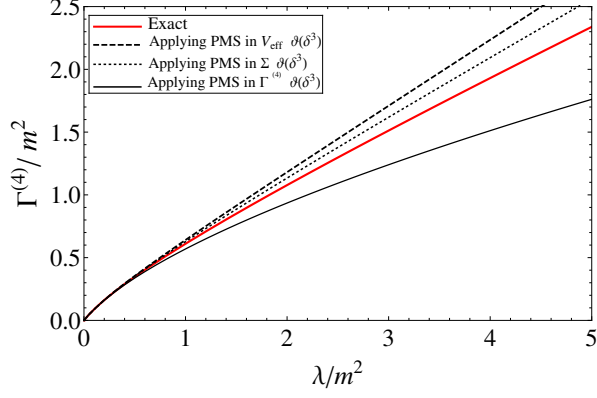


Figure 10: Exact (solid line) and OPT results up to $\mathcal{O}(\delta^3)$ for the 1PI four point function $\Gamma^{(4)}$ at $N = 2$.

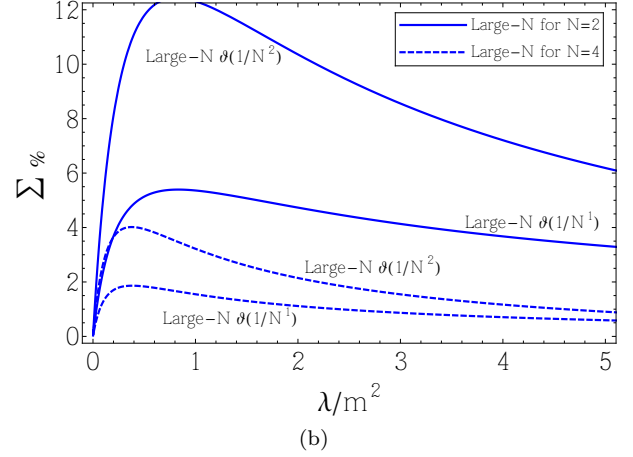
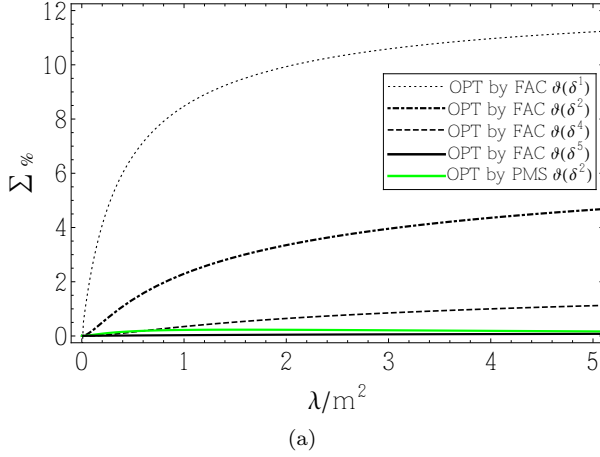


Figure 11: Percentage difference for the Σ . Panel (a): OPT results for $N = 2$ obtained by optimizing Σ by FAC (up to $\mathcal{O}(\delta^5)$) and PMS (up to $\mathcal{O}(\delta^2)$). Panel (b): LN results for $N = 2$ and $N = 4$.

$$\begin{aligned}
\frac{\Sigma}{m} = & \frac{N+2}{6} \left(\frac{\lambda}{m^2}\right)^1 - \frac{N^2+6N+8}{36} \left(\frac{\lambda}{m^2}\right)^2 + \frac{N^3+11N^2+38N+40}{108} \left(\frac{\lambda}{m^2}\right)^3 \\
& - \frac{5N^4+84N^3+512N^2+1320N+1184}{1296} \left(\frac{\lambda}{m^2}\right)^4 \\
& + \frac{7N^5+163N^4+1492N^3+6640N^2+14152N+11296}{3888} \left(\frac{\lambda}{m^2}\right)^5 \\
& - \frac{21N^6+638N^5+8020N^4+53000N^3+192292N^2+357680N+261185}{23328} \left(\frac{\lambda}{m^2}\right)^6 + \mathcal{O}\left(\left(\frac{\lambda}{m^2}\right)^7\right), \quad (\text{A2})
\end{aligned}$$

and

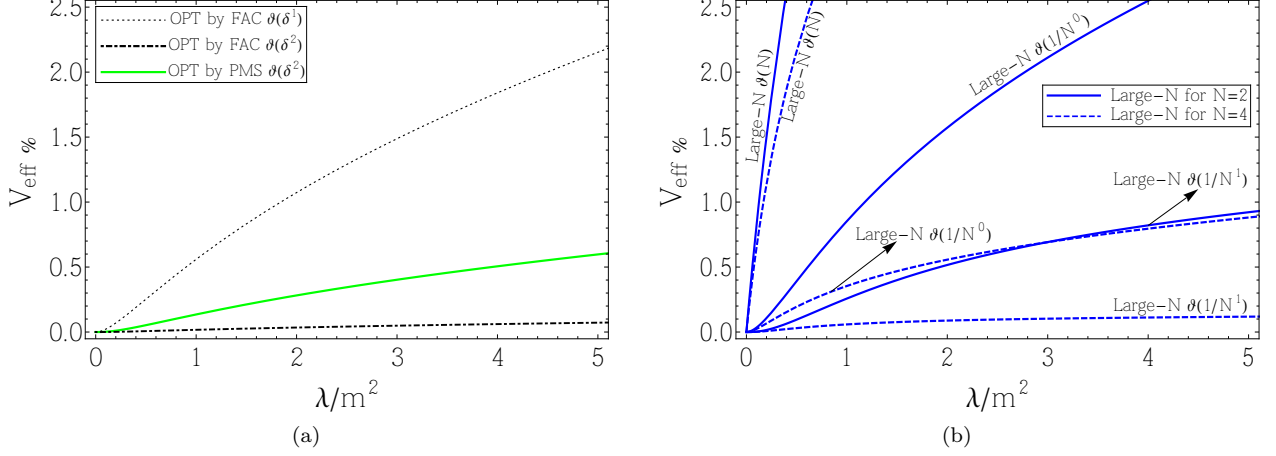


Figure 12: Percentage difference for the V_{eff} . Panel (a): OPT results for $N = 2$ obtained by optimizing Σ by PMS and FAC. Panel (b): LN results for $N = 2$ and $N = 4$.

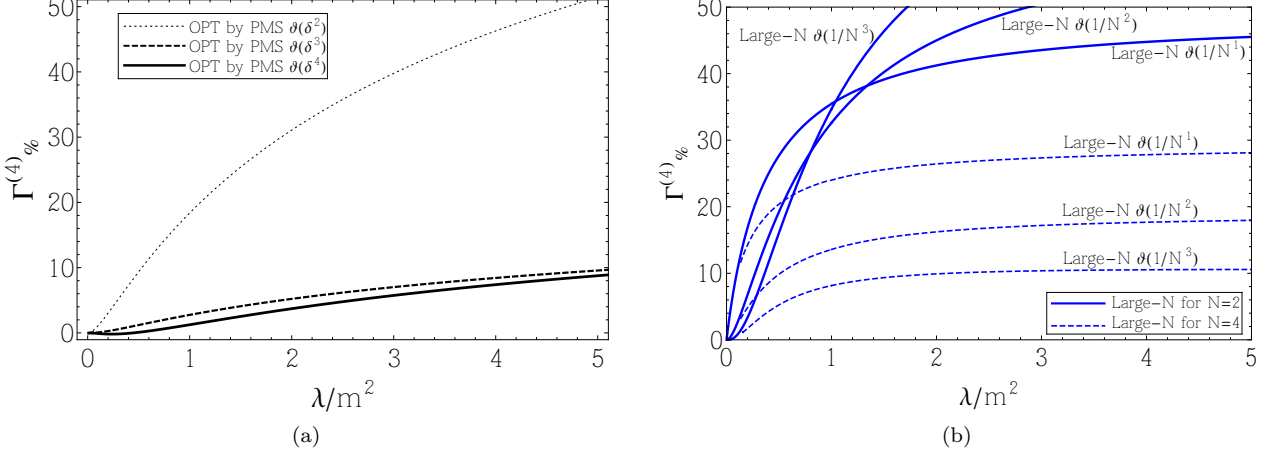


Figure 13: Percentage difference for the $\Gamma^{(4)}$. Panel (a): OPT results for $N = 2$ obtained by optimizing Σ by PMS. Panel (b): LN results for $N = 2$ and $N = 4$.

$$\begin{aligned}
\frac{\Gamma^{(4)}}{m^2} &= \left(\frac{\lambda}{m^2}\right)^1 - \frac{N+8}{6} \left(\frac{\lambda}{m^2}\right)^2 + \frac{3N^2+46N+140}{36} \left(\frac{\lambda}{m^2}\right)^3 \\
&\quad - \frac{5N^3+117N^2+772N+1536}{108} \left(\frac{\lambda}{m^2}\right)^4 \\
&\quad + \frac{35N^4+1124N^3+11880N^2+51568N+79168}{1296} \left(\frac{\lambda}{m^2}\right)^5 \\
&\quad - \frac{63N^5+2609N^4+38874N^3+271676N^2+906576N+1164032}{3888} \left(\frac{\lambda}{m^2}\right)^6 + \mathcal{O}\left(\left(\frac{\lambda}{m^2}\right)^7\right). \quad (\text{A3})
\end{aligned}$$

Appendix B: High order terms in the OPT

In this appendix we present the results obtained for the OPT when expanded up to order $\delta^{(5)}$ for effective poten-

tial V_{eff} , for the self-energy Σ and for the 1PI four-point

Green function $\Gamma^{(4)}$. These results are obtained following the perturbative expansion in terms of the parameter δ ,

using as interaction term Eq. (3.4). The expressions for V_{eff} , Σ and $\Gamma^{(4)}$ are given, respectively, by

$$\begin{aligned}
V_{\text{eff}} = & -\ln \left[\frac{2^{N-1} \pi^{N/2}}{(m+\eta)^{N/2}} \right] \delta^0 + \frac{\lambda(2N+N^2) - 12N\eta(m+\eta)}{24(m+\eta)^2} \delta^1 \\
& + \frac{-\lambda^2(6N+5N^2+N^3) + \lambda\eta(24N+12N^2)(m+\eta) - \eta^2 36N(m+\eta)^2}{144(m+\eta)^4} \delta^2 \\
& + \left[\frac{\lambda^3(120N+128N^2+44N^3+5N^4) - \lambda^2\eta(432+36N^2+72N^3)(m+\eta)}{2592(m+\eta)^6} \right. \\
& + \left. \frac{\lambda\eta^2(648N+324N^2)(m+\eta)^2 - \eta^3 N}{2592(m+\eta)^6} - \frac{\eta^3 N}{6(m+\eta)^3} \right] \delta^3 + \left[\frac{-\lambda^4(840N+1040N^2+468N^3+93N^4+7N^5)}{10368(m+\eta)^8} \right. \\
& + \left. \frac{\lambda^3\eta(120N+128N^2+44N^3+5N^4)}{432(m+\eta)^7} - \frac{\lambda^2\eta^2(30N+25N^2+5N^3)}{72(m+\eta)^6} + \frac{\lambda\eta^3(2N+N^2)}{6(m+\eta)^5} - \frac{\eta^4 N}{8(m+\eta)^4} \right] \delta^4 \\
& + \left[\frac{\lambda^5(15120N+20712N^2+11000N^3+2900N^4+386N^5+21N^6)}{77760(m+\eta)^{10}} \right. \\
& - \left. \frac{\lambda^4\eta(840N+1040N^2+468N^3+93N^4+7N^5)}{1296(m+\eta)^9} - \frac{\lambda^2\eta^3(30N+25N^2+5N^3)}{36(m+\eta)^7} \right. \\
& + \left. \frac{\lambda^3\eta^2(840N+896N^2+308N^3+35N^4)}{864(m+\eta)^8} + \frac{\lambda\eta^4(10N+5N^2)}{24(m+\eta)^6} - \frac{\eta^5 N}{10(m+\eta)^5} \right] \delta^5 + \mathcal{O}(\delta^{(6)}), \tag{B1}
\end{aligned}$$

$$\begin{aligned}
\frac{\Sigma}{m} = & \frac{\eta}{m} \delta^0 + \frac{\lambda(2+N) - 6\eta(m+\eta)}{6m(m+\eta)} \delta^1 - \frac{\lambda^2(8+6N+N^2) - \lambda\eta(12N+6N)(m+\eta)^2}{36m(m+\eta)^3} \delta^2 \\
& + \frac{\lambda^3(40+38N+11N^2+N^3) - \lambda^2\eta(72+54N+9N^2)(m+\eta) + \lambda\eta^2(36+18N)(m+\eta)^2}{108m(m+\eta)^5} \delta^3 \\
& - \left[\frac{\lambda^4(1184+1320N+512N^2+84N^3+5N^4) - \lambda^3\eta(2400+2280N+660N^2+60N^3)(m+\eta)}{1296m(m+\eta)^7} \right. \\
& + \left. \frac{\lambda^2\eta^2(8+6N+N^2)}{6m(m+\eta)^5} - \frac{\lambda\eta^3(2+N)}{6m(m+\eta)^4} \right] \delta^4 - \left[\frac{\lambda^5(11296+14152N+6640N^2+1492N^3+163N^4+7N^5)}{3888m(m+\eta)^9} \right. \\
& - \left. \frac{\lambda^4\eta(8288+9240N+3584N^2+588N^3+35N^4)}{1296m(m+\eta)^8} \right. \\
& + \left. \frac{\lambda^3\eta^2(200+190N+55N^2+5N^3)}{36m(m+\eta)^7} - \frac{\lambda^2\eta^3(40+30N+5N^2)}{18m(m+\eta)^6} + \frac{\lambda\eta^4(2+N)}{6m(m+\eta)^5} \right] \delta^5 + \mathcal{O}(\delta^{(6)}), \tag{B2}
\end{aligned}$$

and

$$\begin{aligned}
\frac{\Gamma^{(4)}}{m^2} = & \frac{\lambda}{m^2} \delta^1 - \frac{\lambda^2(8+N)}{6m^2(m+\eta)^2} \delta^2 + \frac{\lambda^3(140+46N+3N^2) - \lambda^2\eta(96+12N)(m+\eta)}{36m^2(m+\eta)^4} \delta^3 \\
& - \left[\frac{\lambda^4(1536+1772N+117N^2+5N^3)}{108m^2(m+\eta)^6} - \frac{\lambda^3\eta(140+46N+3N^2)}{9m^2(m+\eta)^5} + \frac{\lambda^2\eta^2(8+N)}{2m^2(m+\eta)^4} \right] \delta^4 \\
& + \left[\frac{\lambda^5(79168+51568N+11880N^2+1124N^3+35N^4)}{1296m^2(m+\eta)^8} - \frac{\lambda^4\eta(1136+772N+1117N^2+5N^3)}{18m^2(m+\eta)^7} \right. \\
& + \left. \frac{\lambda^3\eta^2(700+230N+15N^2)}{18m^2(m+\eta)^6} - \frac{\lambda^2\eta^3(16+2N)}{3m^2(m+\eta)^5} \right] \delta^5 + \mathcal{O}(\delta^{(6)}). \tag{B3}
\end{aligned}$$

Appendix C: Large- N Approximation

Ref. [27]. In this appendix we reproduce some of the ex-

The LN approximation applied for the 0-dimensional $O(N)$ scalar field model was described in details in

pressions obtained from that reference that we have used in this work. For this model, we have that $\varphi^2 = \mathcal{O}(N)$ and $\lambda = \mathcal{O}(1/N)$, which shows that $\lambda \rightarrow \tilde{\lambda}/N$ is a reasonable replacement. In the large- N limit we can evaluate the partition function Z in the saddle-point approximation [40] (leading and next-to-leading orders terms).

Performing the change of variables ($y = \frac{\varphi^2}{N}$) and using hyperspherical coordinates we can evaluate the partition function that can be written as

$$Z = \Omega_N N^{N/2} \int_0^\infty \frac{dy}{2y} e^{-Nf(y)}, \quad (\text{C1})$$

where the function $f(y)$ is defined by

$$f(y) = \frac{m}{2}y + \frac{\tilde{\lambda}}{4!}y^2 - \frac{1}{2}\ln(y). \quad (\text{C2})$$

In a saddle point approximation we perform an expansion in Eq. (C2) around its minimum,

$$y_0 = \frac{3m}{\tilde{\lambda}} \left(\sqrt{1 + \frac{2\tilde{\lambda}}{3m^2}} - 1 \right). \quad (\text{C3})$$

Expanding around this minimum and performing the integral, we obtain the partition function [27]

$$Z = \Omega_N N^{\frac{N}{2}} e^{-Nf(y_0)} \left(\frac{1}{4y_0^2} \frac{2\pi}{f''(y_0)} \right)^{1/2} \times \left[1 + \frac{12m^2y_0^2 - 27my_0 + 16}{6N(2 - my_0)^3} \right] [1 + \mathcal{O}(1/N)] \quad (\text{C4})$$

with

$$f(y_0) = \frac{my_0}{4} + \frac{1}{4} - \frac{1}{2}\ln(y_0). \quad (\text{C5})$$

Next-to-leading order LN results for $\Gamma^{(0)}$ can be obtained by taking the logarithm of $\frac{Z}{Z_0}$:

$$\Gamma^{(0)} = \left[\frac{my_0}{4} - \frac{1}{4} - \frac{1}{2}\log(my_0) \right] N^1 + \frac{1}{2}\log(2 - my_0)N^0 - \frac{(8 + my_0)(my_0 - 1)^2}{6(2 - my_0)^3} \frac{1}{N^1} + \mathcal{O}(1/N^2). \quad (\text{C6})$$

Higher order terms in $1/N$ usually are very difficult to obtain because we need go beyond the saddle-point approximation, including fluctuations in the corrections. But for the case of the 0-dimensional $O(N)$ scalar field model, it can be obtained by successive derivatives of $\Gamma^{(0)}$ with respect to m . Following this procedure, we can for the self-energy the result

$$\Sigma = \left[\frac{1}{y_0} - m \right] \frac{1}{N^0} + \left[\frac{2(1 - my_0)}{y_0(2 - my_0)^2} \right] \frac{1}{N^1} + \left[\frac{4(my_0 - 1)^2(3my_0 - 1)}{y_0(2 - my_0)^5} \right] \frac{1}{N^2} + \mathcal{O}(1/N^3), \quad (\text{C7})$$

and also for the 1PI four-point function,

$$\Gamma^{(4)} = \left[\frac{6(1 - my_0)}{y_0^2(2 - my_0)} \right] \frac{1}{N} - \left[\frac{12(1 - my_0)^2(m^2y_0^2 - 3my_0 + 6)}{y_0^2(2 - my_0)^4} \right] \frac{1}{N^2} + \left[\frac{24(1 - my_0)^3}{y_0^2(2 - my_0)^7} \right] \frac{1}{N^3} \times (m^4y_0^4 - 8m^3y_0^3 + 35m^2y_0^2 - 49my_0 + 56) + \mathcal{O}(1/N^4). \quad (\text{C8})$$

-
- [1] D. J. Gross, R. D. Pisarski and L. G. Yaffe, Rev. Mod. Phys. **53** (1981) 43. doi:10.1103/RevModPhys.53.43 doi:10.1103/RevModPhys.53.43;
- [2] J. R. Espinosa, M. Quiros and F. Zwirner, Phys. Lett. B **291** (1992) 115 doi:10.1016/0370-2693(92)90129-R [hep-ph/9206227].
- [3] M. Gleiser and R. O. Ramos, Phys. Lett. B **300** (1993) 271 doi:10.1016/0370-2693(93)90365-O [hep-ph/9211219].
- [4] M. Moshe and J. Zinn-Justin, Phys. Rept. **385** (2003) 69 doi:10.1016/S0370-1573(03)00263-1 [hep-th/0306133].
- [5] A. Okopinska, Phys. Rev. D **35** (1987) 1835. doi:10.1103/PhysRevD.35.1835
- [6] S. Gandhi and M. B. Pinto, Phys. Rev. D **46**, 2570 (1992).
- [7] H. Yamada, Z. Phys. C **59**, 67 (1993).
- [8] K. G. Klimenko, Z. Phys. C **60**, 677 (1993).
- [9] J.-L. Kneur, M. B. Pinto and R. O. Ramos, Phys. Rev. A **68**, 043615 (2003).
- [10] M. B. Pinto, R. O. Ramos, and P. J. Sena, Phys. A **342** 570, (2004).
- [11] R. L. S. Farias, G. Krein and R. O. Ramos, Phys. Rev. D **78**, 065046 (2008).
- [12] M. C. B. Abdalla, J. A. Helayel-Neto, D.L. Nedel, and C.R. Senise, Jr., Phys. Rev. D **77**, 125020 (2008).
- [13] D. C. Duarte, R. L. S. Farias and R. O. Ramos, Phys. Rev. D **84**, 083525 (2011).
- [14] M.C.B. Abdalla, R.L.S. Farias, J.A. Helayel-Neto, D.L. Nedel, C.R. Senise, Jr, Phys. Rev. D **86**, 085024 (2012).
- [15] S. Chiku and T. Hatsuda, Phys. Rev. D **58**, 076001

- (1998).
- [16] S. Chiku, Prog. Theor. Phys. **104**, 1129 (2000).
- [17] E. Braaten and E. Radescu, Phys. Rev. Lett. **89**, 271602 (2002).
- [18] H. Kleinert and W. Janke, Phys. Lett. A **206**, 283 (1995); H. Kleinert, Phys. Rev. D **57**, 2264 (1998); R. P. Feynman and H. Kleinert, Phys. Rev. A **34**, 5080 (1986).
- [19] V.I. Yukalov, Moscow Univ. Phys. Bull. **31**, 10 (1976); Theor. Math. Phys. **28**, 652 (1976); V. I. Yukalov and E. P. Yukalova, Ann. Phys. **277**, 219 (1999); Chaos Solitons Fractals **14**, 839 (2002).
- [20] I. R. C. Buckley, A. Duncan and H. F. Jones, Phys. Rev. D **47**, 2554 (1993); C. M. Bender, A. Duncan and H. F. Jones, Phys. Rev. D **49**, 4219 (1994); C. Arvanitis, H. F. Jones and C. S. Parker, Phys. Rev. D **52**, 3704 (1995).
- [21] J.O. Andersen, E. Braaten and M. Strickland, Phys. Rev. D **63**, 105008 (2001).
- [22] P. M. Stevenson, Phys. Rev. D **23** (1981) 2916. doi:10.1103/PhysRevD.23.2916
- [23] G. Krein, D. P. Menezes and M. B. Pinto, Phys. Lett. B **370** (1996) 5 doi:10.1016/0370-2693(95)01578-7 [nucl-th/9510059].
- [24] J. L. Kneur, M. B. Pinto and R. O. Ramos, Phys. Rev. D **74** (2006) 125020 doi:10.1103/PhysRevD.74.125020 [hep-th/0610201]. J. L. Kneur, M. B. Pinto, R. O. Ramos and E. Staudt, Phys. Lett. B **657** (2007) 136 doi:10.1016/j.physletb.2007.10.013 [arXiv:0705.0673 [hep-ph]]. J. L. Kneur, M. B. Pinto and R. O. Ramos, Phys. Rev. C **81** (2010) 065205 doi:10.1103/PhysRevC.81.065205 [arXiv:1004.3815 [hep-ph]].
- [25] M. B. Pinto and R. O. Ramos, Phys. Rev. D **60** (1999) 105005 doi:10.1103/PhysRevD.60.105005 [hep-ph/9903353].
- [26] M. B. Pinto and R. O. Ramos, Phys. Rev. D **61** (2000) 125016 doi:10.1103/PhysRevD.61.125016 [hep-ph/9912273].
- [27] J. Keitel and L. Bartosch, J. Phys. A **45** (2012) 105401 doi:10.1088/1751-8113/45/10/105401 [arXiv:1109.3013 [cond-mat.stat-mech]].
- [28] P. Ramond, *Field Theory: A Modern Primer* (Addison-Wesely, 1990).
- [29] G. Huber, A. Math. Mon. **89**, 301 (1982).
- [30] *Handbook of Mathematical Functions*, edited by M. Abramowitz and I. A. Steigen (Dover, New York, 1972), 9th ed.
- [31] H. Kleinert, V. Schulte-Frohlinde, *Critical Properties of Φ^4 -Theories*, 1th Edition (World scientific Pub Co Inc, Singapore, 2001).
- [32] I. R. C. Buckley, A. Duncan and H. F. Jones, Phys. Rev. D **47**, 2554 (1993);
- [33] B. Bellet, P. Garcia and A. Neveu, Int. J. Mod. Phys. A **11**, 5587 (1996); **11**, 5607 (1996);
- [34] S. Chiku, Prog. Theor. Phys. **104**, 1129 (2000);
- [35] H. Kleinert and V. I. Yukalov, Phys. Rev. E **71**, 026131 (2005).
- [36] J. L. Kneur, M. B. Pinto and R. O. Ramos, Phys. Rev. Lett. **89** (2002) 210403 doi:10.1103/PhysRevLett.89.210403 [cond-mat/0207089].
- [37] J. L. Kneur and A. Neveu, Phys. Rev. D **88** (2013) 074025 doi:10.1103/PhysRevD.88.074025 [arXiv:1305.6910 [hep-ph]].
- [38] J.-L. Kneur and M. B. Pinto, Phys. Rev. D **92** (2015) 116008 doi:10.1103/PhysRevD.92.116008 [arXiv:1508.02610 [hep-ph]].
- [39] J.-L. Kneur and M. B. Pinto, Phys. Rev. Lett. **116** (2016) 031601 doi:10.1103/PhysRevLett.116.031601 [arXiv:1507.03508 [hep-ph]].
- [40] G. B. Arfken and H. J. Weber, *Mathematical Methods for Physicists*, 6th edition (Academic Press, New York, 2005).